Neutrino telescopes in the Mediterranean Sea.

J. Carr, G. Hallewell

New Journal of Physics
An Institute of Physics and Deutsche Physikalische Gesellschaft Journal

Neutrino telescopes in the Mediterranean Sea

J Carr and G Hallewell

Centre de Physique de Particules de Marseille/IN2P3-CNRS 163 Ave. de Luminy, 13288 Marseille, France
E-mail: gregh@cppm.in2p3.fr and carr@cppm.in2p3.fr

New Journal of Physics **6** (2004) 112
Received 5 May 2004
Published 25 August 2004
Online at http://www.njp.org/
doi:10.1088/1367-2630/6/1/112

Abstract. In the Mediterranean Sea there are three sites where neutrino telescopes are being constructed or developed. The collaborations associated with these sites, ANTARES, NEMO and NESTOR, have adopted different technical solutions to implement a deep-sea detector. For these projects the various detector architectures are presented; the technological choices are compared and the current status is described.

PII: S1367-2630(04)80245-3

Contents

1. Introduction

A number of possible techniques exist to detect high-energy neutrinos from outer space but the most widely exploited method is the detection in large volumes of water or ice of Čerenkov light from the muons and hadrons produced by neutrino interactions with matter around the detector. Water Čerenkov detectors (e.g. IMB, Kamiokande, Super-Kamiokande and SNO) are the only detectors so far to have observed neutrinos produced beyond the earth; these observations being 10^6–10^7 eV neutrinos produced in the sun and supernova 1987a. Experiments are also being developed based on detection of radio wave emission or sound produced in the interactions together with detection of light emission from showers initiated by neutrinos in the atmosphere. These latter techniques are possible for neutrinos with energies above 10^{16} eV. The large sea-based neutrino telescopes described in this paper, as well as the ice-based neutrinos described elsewhere in this review, aim at detection of neutrinos in the 10^{10}–10^{16} eV energy range.

The major scientific objectives of sea-based neutrino telescopes are the discovery and understanding of the sites of acceleration of high-energy particles in the universe. Since their original discovery 100 years ago, the origin of high-energy charged cosmic rays arriving on the earth is unknown. Neutrinos offer a unique possibility to trace cosmic rays back to their origins. Being electric charge neutral they are unperturbed by magnetic fields while, being weakly interacting, they can pass through dense dust clouds which might surround their sources. There are numerous candidate neutrino sources in the cosmos; among the possible sources in the local galaxy are supernova remnants, pulsars and microquasars. Possible extragalactic sources include active galactic nuclei and γ ray bursts. An irreducible background to searches for primary neutrinos from these cosmic sources consists of secondary neutrinos from cosmic ray interactions in the earth's atmosphere.

An important further objective of neutrino telescopes is the search for dark matter in the form of neutralinos. In supersymmetric theories with R-parity conservation, the relic neutralinos from the Big Bang are predicted to concentrate in massive bodies such as the centres of the earth, the sun and the galaxy. At these sites, neutralino annihilations and the subsequent decays of the resulting particles would yield neutrinos detectable in neutrino telescopes of the scale currently in operation and being constructed.

The present paper describes the status of the projects constructing neutrino telescopes in the Mediterranean Sea. Two neutrino telescope projects, ANTARES and NESTOR, are aiming at scientific discoveries with medium-sized detectors while the NEMO project is currently undertaking research and development for the construction of a future larger detector. Sections 1–3 describe the detector techniques and the general concepts of the three projects, section 4 focuses on some technical aspects of the detectors and the concluding sections outline the present status of these projects.

2. Deep-sea neutrino telescopes

A deep sea-water telescope has significant advantages over ice and lake-water experiments due to the better optical properties of the medium. However, serious technological challenges must be overcome to deploy and operate a detector in the deep sea. The pioneering sea-water project, DUMAND, which worked from 1980 to 1995 to deploy a detector off the coast of Hawaii, did not overcome these challenges and the project was cancelled. In contrast, the projects AMANDA and BAIKAL, which deploy from the solid glacial ice and frozen surface lake ice respectively, have developed workable deployment systems. The advantages of sea-water neutrino telescopes are significantly better angular resolution—less than 0.3° for ANTARES compared with 3° for AMANDA—as well as a more uniform efficiency due to the homogeneous medium. A disadvantage of a sea-water detector is the higher optical background due to radioactive decay of ^{40}K and light emission from living organisms: bioluminescence. These backgrounds can be overcome in the design of the detector by having a higher density of optical modules and high bandwidth data readout.

2.1. Detector concepts and site considerations

A deep-sea neutrino telescope detects neutrinos by observing the Čerenkov light produced by muons in the sea water with the muons originating from interactions of the neutrino in the sea

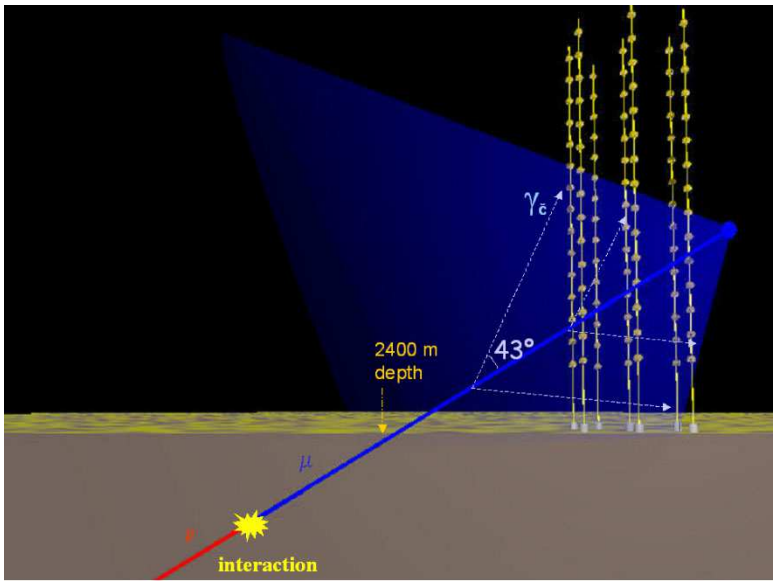

Figure 1. Principle of detection of high-energy neutrinos in an underwater neutrino telescope.

water around the detector or in the rock below it. A matrix of light detectors, in the form of photomultipliers in glass spheres, 'optical modules', is deployed near the seabed. This matrix of light detectors enables the direction of the muon track to be measured with a precision of a few tenths of a degree and at high energies the muon track direction is closely aligned with that of the neutrino such that the neutrino direction is measured with similar precision. Figure 1 illustrates the principle of neutrino detection with the undersea telescope.

The detection of high-energy muon neutrinos exploits three properties:

(i) The directional correlation of the muon and parent neutrino trajectories to within 0.3° for $E_\nu > 10\,\mathrm{TeV}$.

(ii) The unique upward-going directional signature of muons from cosmic neutrino interactions with respect to the vastly higher muon background from cosmic ray collisions in the atmosphere. Upward-going muons can only originate from local neutrino interactions: the earth filters out all other particles.

(iii) The long range of muons in water and rock over the neutrino energy range of interest. Upward-going muons may be generated far from the instrumented volume and still be detected.

Accurate reconstruction of the trajectory of a neutrino-induced muon relies on tracking over many tens of metres and measurement of the arrival time of the UV-blue component of the Čerenkov wavefront to nanosecond accuracy on photomultiplier tubes (PMTs) whose positions must be known to better than 20 cm.

The detection of electron and tau neutrinos is possible in these telescope optimized for muon neutrino detection but except at very high energy the detection efficiency for these other neutrino types is lower.

The choice of the PMT array spacing depends on the absorption and scattering length in the local deep-water environment and to a lesser degree on the limit set by the chromatic dispersion in arrival time of the Čerenkov photons. Due to the high purity of water at great depth, light absorption and scattering are small. However, the detector is subject to backgrounds from cosmic ray muons, luminescence from deep-water creatures and from Čerenkov light from the β disintegration of ^{40}K, present in sea salt.

The criteria for the site of an underwater neutrino observatory are:

(i) Closeness to the coast to ease deployment and reduce the expense of the power and signal cable connections to the shore.

(ii) A sufficient depth to reduce background from atmospheric muons, and to suppress their miss-reconstruction as up-going. A depth of 1000 m is a minimal requirement; the ANTARES site has a depth of 2400 m, the NEMO site 3400 m and the NESTOR site 4100 m.

(iii) Good optical properties in water: long absorption ($>$20 m) and scattering ($\sim$50 m) lengths[1] for light in the range ($350 < \lambda < 550$ nm).

(iv) Low level of bioluminescence.

(v) Low rates of biofouling (bacterial film deposition and marine life accretion) on optical surfaces.

(vi) Low rates of sedimentation (for any upward-looking optical components).

(vii) Low velocity bottom current ($\sim$few cm s^{-1}), since rate of bioluminescence is dependent on this parameter.

3. Mediterranean Neutrino Telescope projects

In the Mediterranean Sea, three sites are under evaluation for Neutrino Telescope projects at the locations shown in figure 2. The most advanced project is that of the ANTARES collaboration which is building a detector with initially 900 optical modules and effective area 50 000 m^2 at a site off the south coast of France near Toulon. The NEMO collaboration is exploring a site off Sicily. Since 2000 the ANTARES and NEMO collaborations have been working together on the detector at the Toulon site with an agreement to choose the optimal site in the Mediterranean for a future larger telescope. In addition, the NEMO group has a test site in the bay of Catania used to perform R&D for the future large detector. The NESTOR collaboration intends to build a detector with 168 optical modules and around 20 000 m^2 effective area at a site near Pylos off the coast of Greece. The different projects have chosen different solutions for the technical implementation of the deep-sea neutrino telescope concept.

The ANTARES collaboration started in 1996 to explore sites off the French coast. The site chosen is at 42°50′N 6°10′E with a depth of 2400 m. The ANTARES detector array will suspend optical modules on individual mooring lines, with readout via cables connected to the bottom of the lines. This configuration is similar to that originally chosen by the DUMAND collaboration.

As with DUMAND, the ANTARES detector requires connections to be made on the seabed by underwater vehicles. However, in the last 10 years, the relevant underwater technology has

[1] The absorption coefficient, a, is defined as $1/L_a$; the scattering coefficient, $b = 1/L_b$. Their combination, $c = (L_a + L_b)/(L_a \cdot L_b)$, is the attenuation coefficient. Due to the combination of absorption and scattering phenomena, light intensity scales with distance L as $I = (I_0/L^2)\mathrm{e}^{-cx}$.

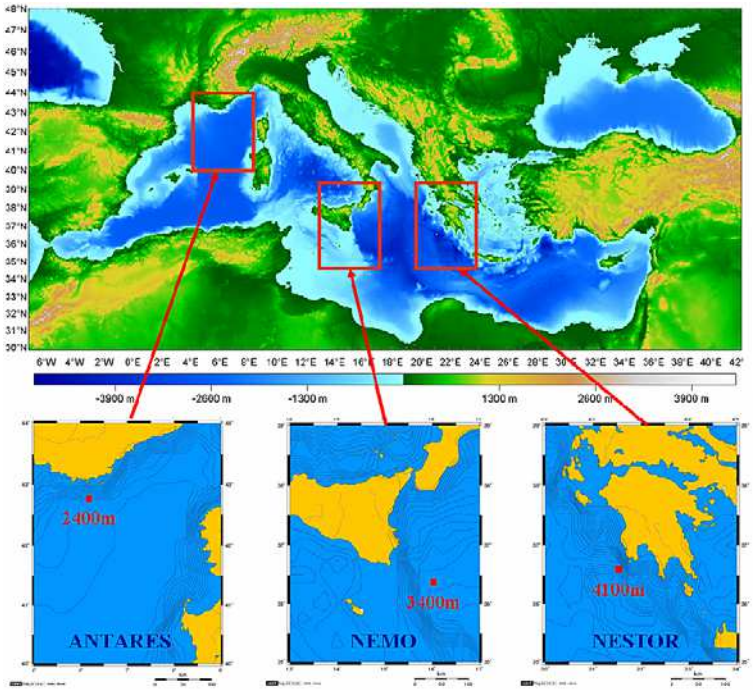

Figure 2. Locations of the sites of the three Mediterranean Neutrino Telescope projects.

advanced significantly due to the needs of the offshore-oil industry, facilitating the ANTARES configuration. Currently, a wide range of suitable deep-sea connectors is available and extensively used in industry, including electro-optical connectors wet mateable at depth on the site. Many commercial underwater vehicles now exist that are capable of making these connections. The ANTARES readout design maximizes the reliability of the detector by dividing the system into independent sections such that the failure of no single active component can cause the loss of the whole detector. The detector signals are digitized in local electronics and transmitted to the shore over high bandwidth optical links. On shore, a computer farm will take the trigger decisions to decide which data are recorded on tape. An advantage of the ANTARES approach is the possibility to quickly recover and repair all elements of the detector deployed in the sea.

The NESTOR detector will be installed at a depth of 4100 m. A key concept of the NESTOR project, and a significant difference with ANTARES, is the arrangement of the optical modules on a tower structure with all internal connections made on the surface during deployment, hereby avoiding the need for underwater connections. The NESTOR towers will contain 12 hexagonal floors of 16 m radius with photomultipliers looking both upward and downward. Test deployments have been performed and many detector elements exist, including the data/power cable connection from the site to the shore.

3.1. ANTARES detector architecture

The geometrical layout and readout architecture of the ANTARES detector have been optimized using four criteria: total detection efficiency, neutrino direction precision and background rejection and cost.

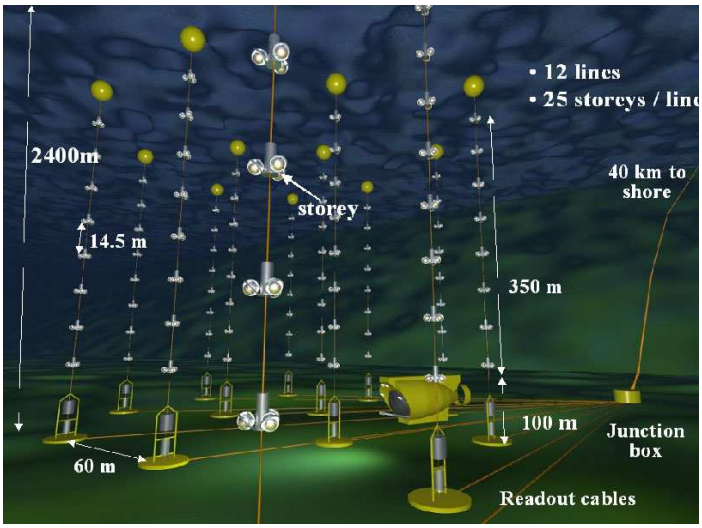

Figure 3. The layout of the ANTARES Neutrino Telescope on the sea floor.

The maximum detection efficiency requires the maximum instrumented volume and is optimal with a homogeneous distribution of light detectors; a configuration which also assures the best precision on neutrino direction. The background reduction requires optical modules closely spaced enough to be able to recognize tracks by timing associations within the distribution of random hits due to the light backgrounds in the sea water from radioactive decays in ^{40}K and bioluminescence. Cost considerations also lead to a close grouping of the light detectors.

The detector geometry chosen by ANTARES is a compromise between the homogenous spacing indicated by the efficiency and precision criteria and the clustering indicated by the background and cost criteria. The layout of the detector is shown in figure 3. The optical modules are arranged in groups of three on lines with a total height of 420 m, which are weighted to the seabed and held nearly vertical by syntactic foam buoys at the top. The seabed at the site is at a depth of 2400 m and the optical modules positioned at depths between 2300 and 2000 m. A line has a total of 75 optical modules arranged in 25 storeys containing three light detectors.

The default readout mode of ANTARES is to transmit the time and amplitude of any light signal above a threshold corresponding to 1/3 of a photo-electron for each optical module. These signals are then treated in a computer farm on shore to find hit patterns corresponding to physics events. The grouping of three optical modules in a storey allows local coincidences to be made for this pattern finding and also, under certain circumstances, local triggers to be formed to reduce the readout rate. The bioluminescence rate at the site varies with season. It is planned that when the singles rate is too high for the throughput of the data acquisition system the local trigger will be used to reduce the data flow to acceptable levels. In addition, the front-end electronics allows a more detailed readout of the light signal than the standard time and amplitude mode. With this detailed readout it is possible to sample the full waveform of the signal with 128 samples separated by $\sim$2 ns, enabling special calibration studies of the electronics.

The readout architecture of the detector has several levels of multiplexing of the photomultiplier signals. The first level is in the 'local control module' (LCM) in each storey of the detector, where the analogue electrical outputs of the photomultipliers are digitized in a

custom-built ASIC chip, the analogue ring sampler (ARS) before being treated by a data acquisition card containing an FPGA and microprocessor, which outputs the multiplexed signals of the three local optical modules on an Ethemet optical link. These links from five storeys, forming a 'Sector', are combined in an Ethemet switch in the master local control module (MLCM) at every fifth storey and the combined link output is sent on a particular wavelength to a dense wavelength division multiplexing (DWDM) system in an electronics container, the string control module (SCM) at the bottom of each line. In the SCM, the outputs from the five MLCMs along the line are multiplexed on to one pair of optical fibres. These fibres are then connected to a junction box on the seabed via interlink cables. In the junction box the outputs from up to 16 lines are gathered onto a 48 fibre electro-optical submarine cable and sent to the experiment shore station at La Seyne-sur-Mer. The optical links between each MLCM and the shore station are connected using only passive components.

The electrical supply system has a similar architecture to the readout system. The submarine cable supplies up to 4400 V, 10 A ac to a transformer in the junction box. The 16 independent secondary outputs from the transformer provide up to 500 V, 4 A to the lines via the interlink cables. At the base of each line a string power module (SPM) power supply shares the same container as the SCM. The SPM distributes up to 400 V dc to the MLCMs and LCMs in each storey each of which contains a local power box (LPB) to provide the various low voltages required by each electronics card.

The 45 km electro-optical undersea cable[2] linking the detector to the shore station was laid in October 2001. The cable was terminated in December 2002 with the deployment of the central electro-optical junction box respectively.

A series of site evaluation campaigns has been carried out by the ANTARES collaboration [1, 2]. At the array depth of 2400 m, the expected background rate from atmospheric cosmic ray muons is around 30 Hz. This rate is insignificant in comparison with the ^{40}K β background from sea salt, which adds a singles rate of 60 kHz to each 10-in PMT, or with occasional bio-luminescence, which can peak during short bursts up to MHz rates, and is seasonally and ocean current dependent. Since the PMTs in the ANTARES array will be angled 45° downward towards the seabed, fouling is not a serious problem. The combined signal loss due to bio-deposition and sedimentation has been measured [1] to be less than 2% per year.

The attenuation and scattering lengths in water at the ANTARES site have been measured in several campaigns between 1998 and 2000. At 466 nm, attenuation (scattering) lengths have varied between 45 and 60 m (37 and 79 m). The seasonal variation in these figures is significant, and the ANTARES array will incorporate an 'instrumentation' line which will deploy underwater instruments including transparency and current profile monitors.

The construction of optical modules for 12 detection lines is well advanced. The commissioning of a full readout chain is in progress: a prototype 'sector line' of five optical module triplets was deployed in late 2002 following the deployment of the electro-optical junction box. A site instrumentation line was deployed in early 2003. The commissioning of the array of 12 detection lines is planned for completion in 2006.

The performance of an undersea neutrino detector is characterized by the effective area: the angular resolution and the energy resolution. The effective area is given either as the effective area for muons or the effective area for neutrinos. The latter quantity is most easily used to

[2] Manufactured and deployed by Alcatel.

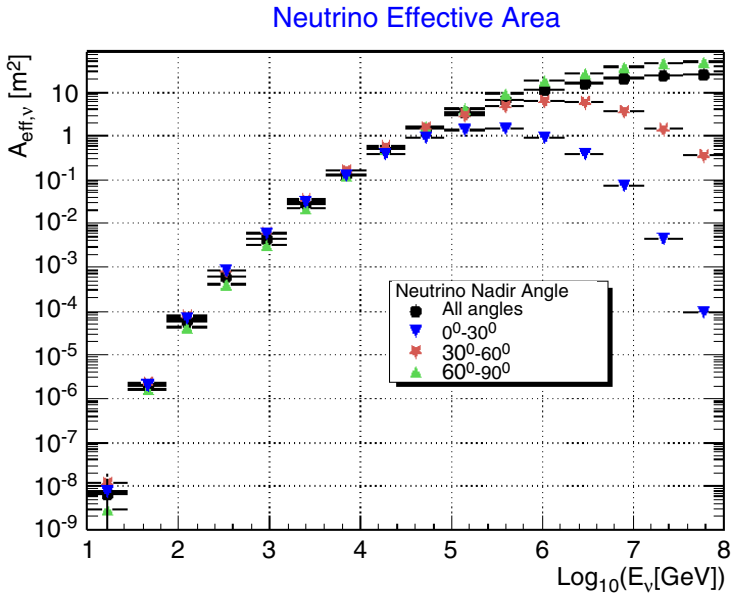

Figure 4. Neutrino effective area for the ANTARES detector as a function of neutrino energy and for various ranges of incident neutrino directions.

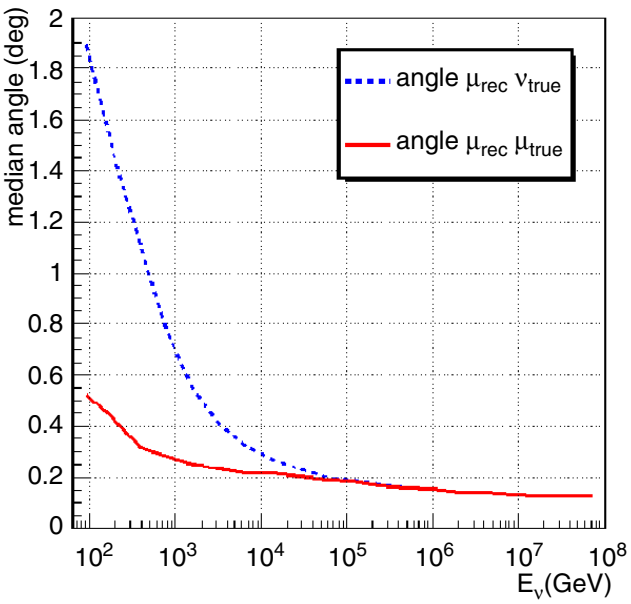

Figure 5. Angular resolution: (red solid line) resolution of the reconstruction of the muon track; (blue dotted line) resolution of the reconstructed muon track relative to the neutrino direction taking into account the kinematics of the neutrino interaction.

calculate the events rates; for this the number of events in the detector is just the product of the neutrino flux and the neutrino effective area. Figure 4 shows the neutrino effective area as simulated for the ANTARES detector. The angular resolution is shown in figure 5 and the energy resolution in figure 6.

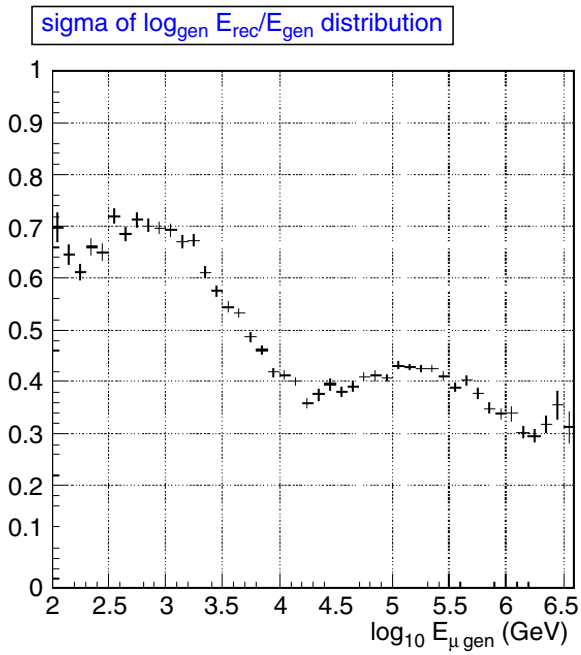

Figure 6. Energy resolution: the value plotted is the sigma of the logarithm of the energy resolution.

3.2. NESTOR detector architecture

The NESTOR array will be located near Pylos on the Greek Ionian Sea coast. An electro-optical cable has been laid from a shore station at Methoni to a site at a depth of 4100 m around 15 km from the shore. The array, shown conceptually in figure 7, will comprise a series of 'towers', each rising 360 m from a seabed anchor, held in tension by an underwater buoy. Each tower will contain 144 PMTs mounted on 12 titanium-framed 32 m diameter 'floors' in the form of six-pointed stars. A pair of PMTs will be mounted on each arm, one looking up and the other down. The array is intended to be installed and extended without the need for underwater electro-optical connections by submarine vehicles.

The water in this region of the Ionian basin is very clear, with ∼55 m attenuation length [3] for blue light. Bottom currents have been measured to be below 10 cm s^{-1}. Extremely low rates of sedimentation and biofouling permit a significant number of upward-looking optical sensors.

The NESTOR cable to shore was deployed in June 2000, but was damaged by the ship during the cable lay. In January 2002 the end of the cable was recovered; the cable was repaired and redeployed at 4100 m with an electro-optical junction box and associated instruments including an underwater current meter, an ocean bottom seismometer, a nephelometer to monitor light scattering, temperature and pressure sensors, a compass and a tilt-meter. Instrument data were transferred to the shore for nearly a year; the first long-duration real-time data readout from a component of deep-sea neutrino detector. The first detector floor was deployed in March 2003 and has allowed the reconstruction of muons as described in section 5.2. After this engineering run, a detector consisting of four floors will be deployed for more tests and physics data taking, followed by the complete tower.

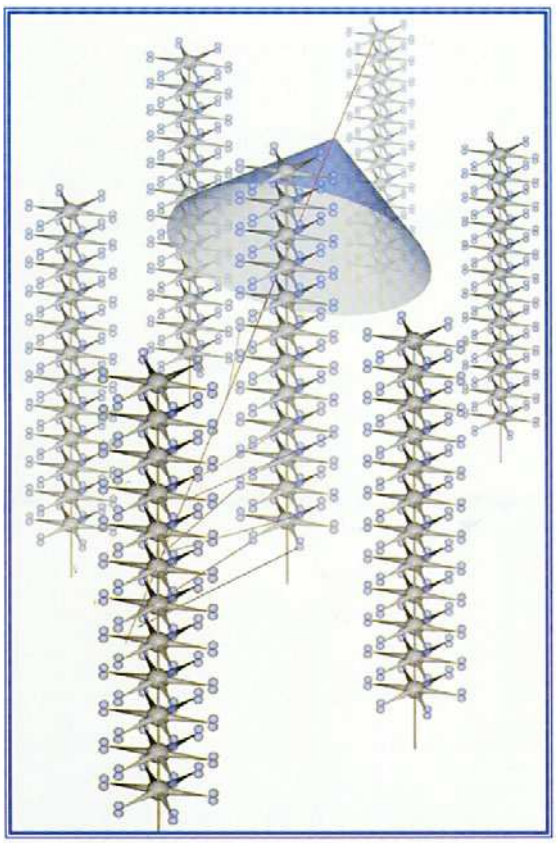

Figure 7. Conceptual layout of the NESTOR array.

3.3. NEMO detector architecture

The NEMO collaboration has identified a possible site for a km^3-scale array at a depth of 3500 m, distant of 80 km from the Sicilian coast near Capo Passero. At this location in the Ionian Sea, bacterial concentration is relatively low, with the consequent advantages of low expected bioluminescence background and biofouling rate. Preliminary studies over a period of 40 days have shown no evidence for biofouling. At the site, the light attenuation (absorption) length exceeds 35 m (70 m) [4]. The average bottom current is around 3 cm s^{-1}, with a measured sedimentation rate of $\sim$20 m g^{-1} d^{-1}. It remains to be proven that this low rate would not seriously degrade the performance of upward-looking PMTs after $\sim$1 year, should the detector design include them.

The NEMO concept is for a 1-km^3-scale array with 4096 optical modules hung from 64 'towers' laid in a square grid with 200 m spacing. Each tower, shown in figure 8, would rise 750 m from a seabed anchor, and would contain 16 'floors' separated in height by 40 m, each with a pair of PMTs at each end of a 20 m composite support arm. A matrix of support cables would ensure that successive floors deploy orthogonally under the force of the suspension buoy. The NEMO collaboration has also brought into service a test site at a depth of 2031 m. A 28 km electro-optical cable from Catania in Sicily [5] splits 23 km from the shore, a second branch running 5 km to the 'Geostar' underwater environmental platform. Each site is serviced by 10 optical fibres and six electrical conductors.

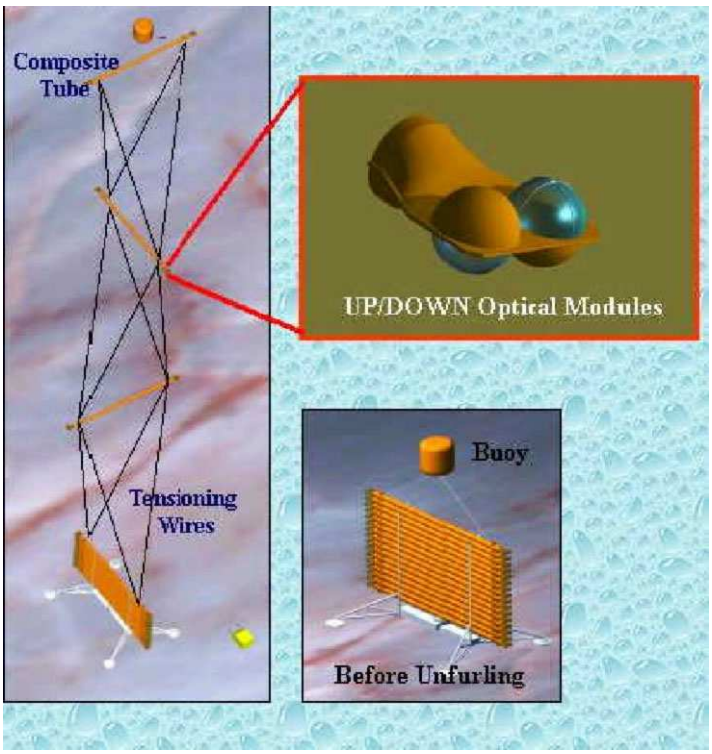

Figure 8. Concept for a NEMO tower.

4. Detector technology issues

In the following sections (see also [6]), the technology of underwater neutrino detectors is discussed in more detail.

4.1. The optical detection modules

As in existing water neutrino detectors such as Super-Kamiokande and SNO, Čerenkov light will be detected using PMTs with single photon sensitivity. The extreme pressure at the operating depths requires that the PMTs be housed in pressure-resistant glass spheres. Such spheres are readily available in diameters up to 43 cm with depth ratings up to 7000 m from several suppliers[3] and may be purchased in a variety of glasses, including low potassium (low β activity) variants. Spheres are supplied as matched hemispheres and can be predrilled with electrical and pump-out penetrations. Leak tightness at high pressures is given by plastic deformation of the ground glass contact surfaces of the hemispheres: no 'O' ring joint is used.

Figure 9 illustrates the components of a generic optical module of an underwater neutrino detector. In ANTARES [7] and NESTOR [8], the pressure spheres from different manufacturers exhibit very similar characteristics: 43 cm diameter with 1.5 cm thick, low activity (<0.5% K content) borosilicate glass having $n = 1.47$ and transmission >87% for $\lambda > 400$ nm. A PMT

[3] Benthos type 2040-17V used in NESTOR (Benthos Corp, North Falmouth, MA 02556, USA), Vitrovex type 8330 used in ANTARES ('Vitrovex' ® by Nautilus Marine Service GmbH, D-28357, Bremen, Germany) and 'EKRAN' (Novosibirsk) and Vitrovex used at Lake Baikal.

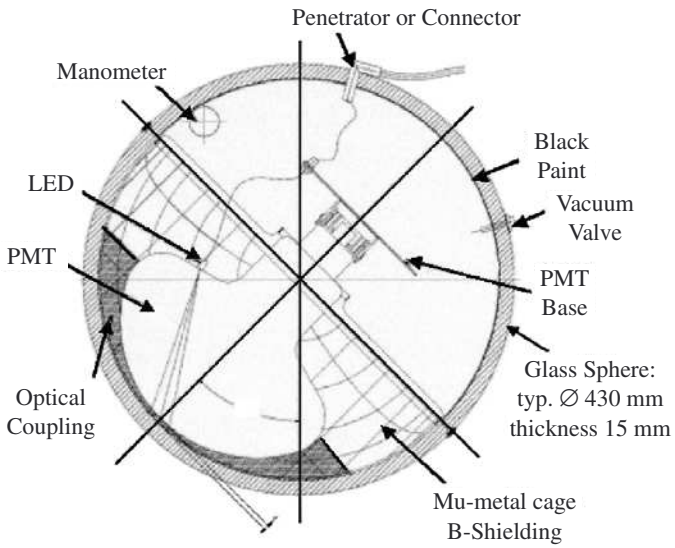

Figure 9. A generic underwater optical module.

Table 1. Parameters of Hamamatsu 7081-20 PMT.

Photocathode-sensitive area	500 cm^2
Combined efficiency (quantum Å collection: $400 < \lambda < 700$ nm)	>16%
Gain at 2500 V	2×10^8
Pulse amplitude at nominal working gain of 5×10^7	60 mV/50 W
Transit time	~60 ns
Transit time spread (TTS: FWHM)	<3 ns
Dark count rate (at 0.3 × single PE threshold)	<10 kHz
Pulse rise time	<5 ns
Pulse width (FWHM: single PE)	<12 ns

with single photon sensitivity is shielded from earth's magnetic field by a two-part mu-metal wire cage, and is mounted and optically coupled onto one hemisphere using an index matching gel.[4] Since power consumption is critical in large detector arrays powered through very long shore cables, the HV bias for the dynode array is usually generated in a custom PMT base from a dc input, using a Cockcroft–Walton chain. A light flasher system consisting of a blue LED and pulser circuit may be added to monitor the PMT transit time, which can exceed 60 ns in large photocathode PMTs. The pulser trigger signal is referenced to the detector master clock.

Table 1 illustrates the performance of the Hamamatsu R7081-20 10-in PMT used by the ANTARES collaboration. Its performance is fairly typical of PMTs used in deep-water neutrino detectors.

[4] In ANTARES, 'Silgel' ® 612 A/B by Wacker-Chemic GmbH (Munich, Germany): two-component silicon rubber, room temperature cure: $n = 1.404$ (transmission >88% for $(400 < \lambda < 700)$ nm). In NESTOR, Wacker Semicosil gel $\{n \sim 1.4\}$ (gel or liquid glycerine, $n = 1.478$) with polyurethane (gel) containment gasket.

Figure 10. Partially folded titanium frame of a NESTOR 'floor' (at NESTOR Institute, Pylos).

4.2. Structural and pressure components

In the present generation of deep underwater neutrino arrays, the requirements of pressure and corrosion resistance have predicated the almost exclusive use of glass and titanium for pressure vessels. Structural supports are in titanium or composites, which will offer important cost savings in km^3-scale arrays. Figures 10, 11 and 12 illustrate the use of titanium in the NESTOR and ANTARES optical module support frames and electro-optical junction box respectively.

Each 32-m-diameter NESTOR titanium floor frame [8, 9] will incorporate a central titanium sphere containing data acquisition, power conversion and monitor and control system electronics. The six arms are composed of folding 5 m tubular frames as shown in figure 10.

Although uncoated ferrous-metal structures (including stainless steel) are unsuitable for use in deep-sea water, possible cost reductions relative to titanium might be achieved by decoupling the problems of pressure and corrosion resistance. Figure 12 illustrates a junction box being considered by NEMO [10] in which a main electro-optical cable is split into parallel outputs for an array of detection lines. Cables exit the walls of the spherical steel pressure vessel through 'penetrators' and pass through an oil volume to terminate in underwater-mateable connectors arranged around the circumference of an oil bath built in composite GRP. An internal flexible water bladder[5] ensures the equi-pressure of water and oil by compensating the slight compressibility of the oil.

4.3. Bottom anchors

The NESTOR, ANTARES and NEMO underwater neutrino detectors tension their detection lines between anchors and a buoy, usually composed of a pressure (compression)-resistant syntactic

[5] Manufactured, for example, by Pronal SA (Leers, France).

Figure 11. Titanium optical module support frames for 'triplet' stories of the ANTARES detector.

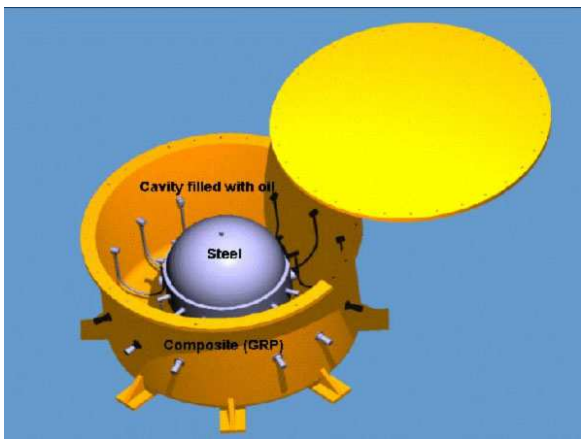

Figure 12. Example of an oil barrier/steel deep-sea junction box pressure vessel (NEMO).

foam.[6] Bottom anchors for deep-water detectors are often sophisticated devices, incorporating an acoustic release system allowing the line to float to the surface for recovery. In this event a 'disposable' deadweight is left on the seabed. In ANTARES and NEMO, an underwater mateable/breakable connector[7] automatically disconnects with the unrestrained line buoyant force.

[6] Glass micro-spheres in resin: manufactured, for example, by BMTI s.a. (La Seyne-sur-Mer, France).
[7] MkII Hybrid (Electro-optical) Connector (Ocean Design Inc, Ormond Beach, FL, USA).

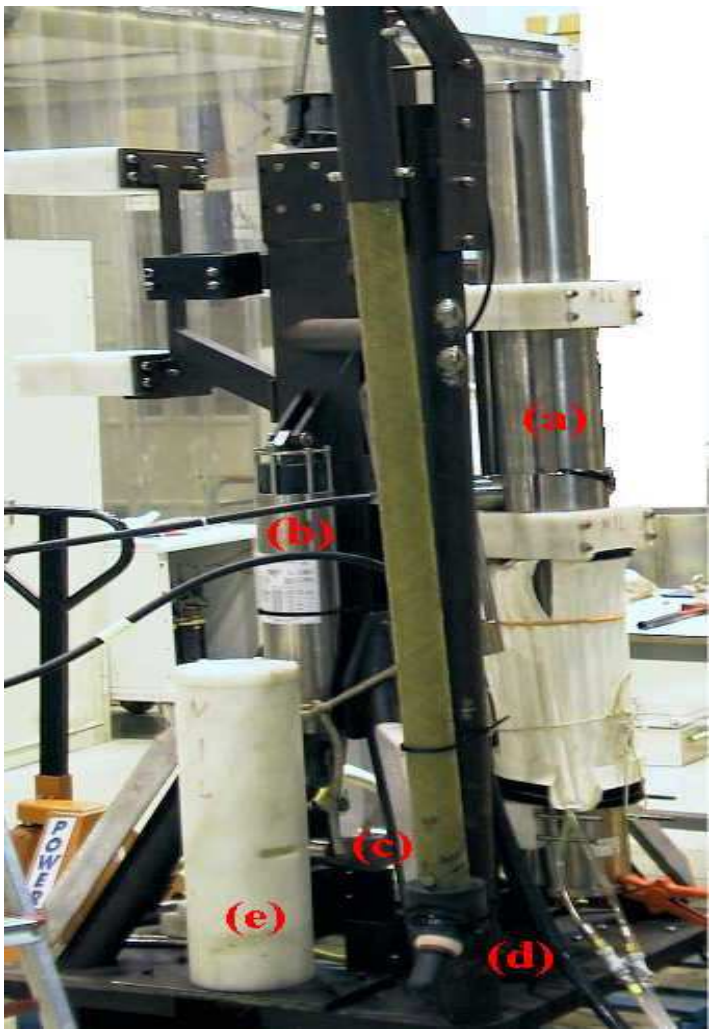

Figure 13. ANTARES 'bottom string socket' anchor.

Figure 13 illustrates the recoverable part of the ANTARES anchor. This incorporates the detection line power converter (a); the acoustically activated release (b) the release shackle (c) and the acoustic survey system transponder[8] (d). The disconnect speed of the underwater-mateable connector is regulated by a pair of sea-water dashpots (e).

4.4. Electro-optical connection and distribution

The present generation underwater neutrino arrays are deployed in stages on sites where an electro-optical shore cable has already been deployed. Unless terminating in deep underwater-mateable connectors, the shore cable must be dredged to the surface for connection to be made to it. Shore cables are deployed with dredging tails and acoustic transponders to enable them to be located for this operation. Options for the connection of additional

[8] Model RT861-B2T (Oceano Technologies, Brest, France; http://www.oceano-technologies.fr).

Figure 14. Example of a commercial (dry-mate) undersea cable electro-optical connector (Photo courtesy Sea Con Inc.).

detector lines are:

(i) Underwater hook-up to the connector on the seabed anchor of a previously deployed line, or more safely, to a previously deployed junction box. Both require the use of underwater-mateable electro-optical connectors and a manned or remotely operated submarine vehicle (ROV). This is the option chosen by ANTARES.

(ii) Deployment of each detection line with a dredgeable or buoy-anchor released cable pigtail of length exceeding the water depth (4–5 km). This allows a dry connection to be made at the surface with less-expensive connectors, without the need for a ROV. This would represent an extension to the present NESTOR recovery/deployment concept using a recoverable rope (ReRo: section 4.8.2), which is not, in its present form, an interlink cable. However, under such a connection strategy, the seabed would risk becoming cluttered with very long cables whose descent would need to be carefully controlled to avoid damage to already-deployed detector elements.

Electro-optical distribution is a significant component of the cost of undersea neutrino detectors, particularly where the shore link cable is long or custom made. In an effort to minimise this cost, ANTARES (NESTOR) have deployed standard telecommunications cables with 48 (18) optical fibres and a *single* power conductor.[9] Figure 14 illustrates the (dry-mateable) electro-optical connector[10] of the ANTARES undersea cable. The connector shell is titanium with an outer diameter of 25 cm. The four electrical contacts (in equipotential in the ANTARES cable) are grouped at the centres. In both detectors, power returns to the shore station via a deep-sea electrode[11] and a shore electrode located below the low tide level. NESTOR uses monopolar dc

[9] In long undersea telephone cables, optical signal repeaters are often powered by series wiring using the single power conductor: one (the other) end station supplying a +ve (−ve) voltage w.r.t. the sea.

[10] SeaCon/Inc, El Cajon, CA, USA.

[11] In ANTARES via a 40-mm diameter titanium bar anode: length 1.7 m with 'KERAMOX®-MMO' coating (Magneto Special Anodes BV, BA Schiedam, Netherlands).

Figure 15. Left: ANTARES junction box with penetrators and underwater-mateable connectors. Right: ANTARES junction box during deployment, illustrating acoustic transponder titanium support frame and undersea cable attachment.

while ANTARES will be powered with 4200 V 50 Hz ac at ∼8 A: a central transformer in an underwater junction box reducing and distributing the voltage to the detector lines.

The ANTARES 50 Hz distribution system is rather conservative and may not be optimal for a km^3-scale detector such that groups are performing R&D for future systems. At the NEMO test site the main electro-optical cable splits into two drops, each with 10 optical fibres and six power conductors [11], which will facilitate studies of a variety of ac and dc powering scenarios.

Figure 15 shows the ANTARES central junction box, which is based on a 1 m diameter titanium sphere with a central cylindrical connector belt through which enter the shore electro-optical cable, the sea electrode cable and 16 'penetrators' with 2.5 m electro-optical cable pigtails ending in underwater-mateable connectors. The junction box is installed in a titanium frame providing strain relief for the re-descent of the shore cable. The frame also contains an acoustic transponder[12] to locate the junction box following deployment.

For undersea connections the Ocean Design MkII Hybrid connector system[13] is used. The receptacle and cable-mounting plug are oil-filled with conductors and fibre ends shuttered in the oil volume in the unmated condition. Upon connection, the shutters open and oil is displaced into bladders at the rear of the receptacle and plug.

The ANTARES junction box is the underwater hub of the detector, splitting the power between the detector lines, distributing clock signals and gathering the data signals from the detector lines onto the shore cable. Its 24 kW transformer has 16 separate 500 V secondaries

[12] Model ET861T by Oceano Technologies: 9 kHz → 14 kHz & v.v.

[13] MkII Hybrid Connector, Titanium shell (2 conductors, 4 fibres). Fibreoptic insertion loss <0.2 dB, HV standoff (pin-shell) 500 V unmated, 1000 V mated (Ocean Design Inc, Ormond Beach, FL 32174, USA). Rated >100 insertions <6000 depth before oil refurbishment.

to power and galvanically isolate each detection or instrumentation line. Each output may be switched on/off or reset by a remotely controllable circuit breaker handled via the triply redundant junction box slow control system. Passive fibre-optic splitters distribute the master clock signals in duplicate to the 16 output lines. Lines will be connected to the junction box as they are deployed, using a ROV equipped with a manipulator arm. Power arriving at a detection line from the junction box is converted from 500 V ac to 380 V dc at the anchor for passage up the cable to the 25 electronic containers. In these, it is further reduced via dc/dc converters for use in optical modules and readout electronics.

Very high reliability is required of critical underwater electronics and power distribution components, MTBF (mean time between failures) $\gg$10 year typical operational life, due to the very high cost of recovery and repair of damaged components, particularly should submarine vehicles be required.

In contrast to the situation with electro-optical connectors, a wider variety of underwater all-electrical or all-fibre connectors exists. Relatively inexpensive dry-mateable types for 500 bar + ambient pressure are available from several manufacturers, including Sea-Con Inc and Gisma.[14]

4.5. Readout systems

The principal problem for the readout systems of undersea neutrino telescopes is the separation of single photoelectron (SPE)-like PMT signals along muon trajectories from background due to ^{40}K disintegrations and PMT dark current pulses and occasional bioluminescence. The bioluminescence rate is very variable in time, pulses lasting a few seconds with rates up to MHz being produced by fish while bacteria and plankton give rates which vary with sea current. Pulses from bioluminescence represent the main contribution to PMT dead time, but these high rates are usually correlated over only a few adjacent PMTs.

Data may be uploaded to the shore with or without the application of local ('off-shore') triggering or local bioluminescence-rejecting coincidences. The 'all-to-shore' option allows trigger decisions to be taken in on-shore electronics which can be upgraded to profit from technology advances during the lifetime of the detector.

4.5.1. The NESTOR data acquisition system. The NESTOR readout [9] and data acquisition system (RDAQ) follows a data-driven architecture with waveform capture and capabilities for forming local (per floor) coincidences to reduce on-shore processing requirements.

Within the central titanium sphere of each floor, a 'floor board' implements PMT pulse sensing, majority logic event triggering, waveform capture and digitization for 12 PMTs. The board extracts data, formats events and transmits data via the single bi-directional optical fibre up-/downlink per floor to the shore. Its FPGA/PLDs can be reprogrammed through the downlink.

The heart of the board is the four-channel analogue transient waveform digitizer (ATWD) ASIC, developed at LBNL. Each channel contains 128 10-bit ADCs, which after activation simultaneously digitize 128 samples of a selected channel. At the chosen sampling rate of 282 MHz, each channel has a time range of 453 ns. One channel in each ATWD is retained for synchronization, digitizing the waveform of a 40 MHz clock signal. A 'shore board' at the

[14] Gisma, Neumuenster, Germany: http://www.gisma-connectors.de.

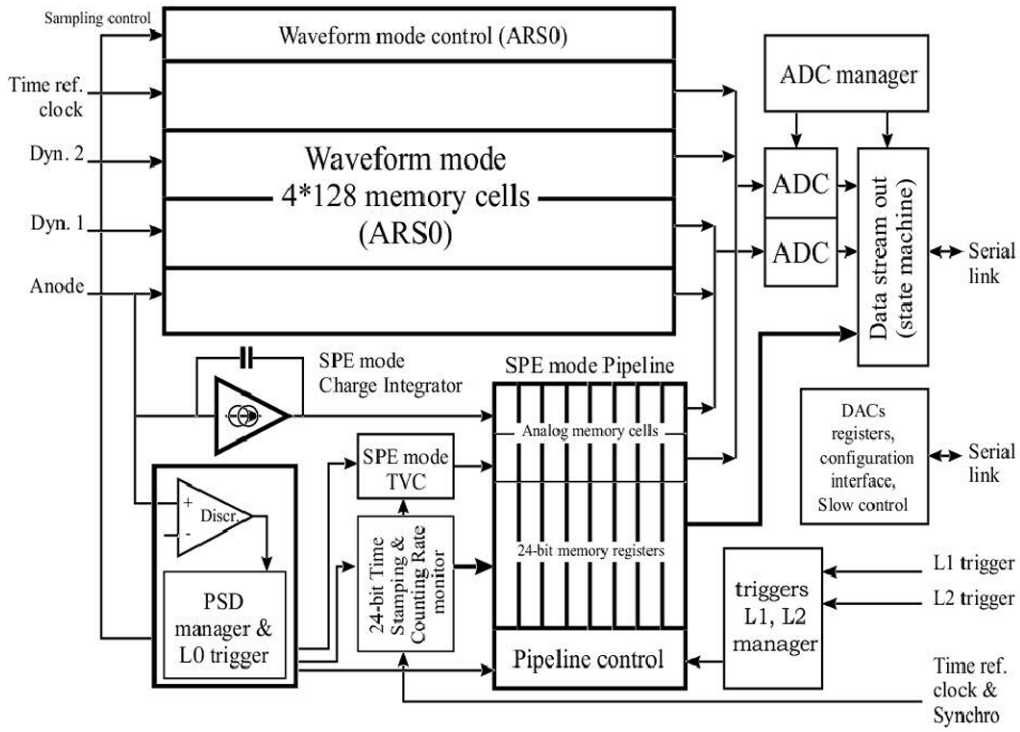

Figure 16. ANTARES ARS functionality.

shore counting room, broadcasts a global 40 MHz clock signal via downlink to the floor board, receives the uplink data and transmits them to the second level triggering system.

A 'floor-trigger' occurs when the programmed local coincidence requirement is satisfied on the floor. The time-stamp of a floor-trigger is defined as the leading edge of the majority logic signal, and the occurrence of such a trigger initiates waveform capture by the ATWD. This time stamp will also be used at the shore to build a global event combining experimental information from several floors.

The performance of the RDAQ electronics and the online software has been extensively studied in the laboratory using an LED calibration system. The robustness of the system has been demonstrated under near-realistic immersion conditions at the NESTOR Navarino Bay Test Station. The rms time stability of ATWD sampling at frequency of 282 MHz has been measured to be 6.4 ps [9], negligible compared with the sampling period of 3.54 ns.

4.5.2. The ANTARES data acquisition system. In the ANTARES array, the functions of the detector readout system are to time-stamp (accepted) analogue PMT signals, to digitize their charge and to merge the data from the 90 PMTs on each detector line onto each single fibre-optic uplink to the shore station. The first stage of PM signal processing is performed by the analogue ring sampler (ARS) ASIC [12] (figure 16). The ARS chips associated with each optical module triplet are housed in a common electronics container, together with (depending on the position of the triplet along the detection line) the compass and tiltmeter and/or hydrophone signal processing cards of the line positioning system.

The ARS ASIC is implemented in AMS 0.8 μm CMOS technology, and is based on a four-channel mixed analogue/digital pipeline memory. The ARS also implements a waveform

shape-sensitive discriminator to distinguish single photoelectron-like (SPE) pulse shapes from superimposed pulses or from larger pulses characteristic of background. The PMT direct anode signal enters one of the four inputs. Although each input can handle pulses up to 4.5 V, an attenuated anode signal, and a signal from the 12th dynode are used to extend dynamic range in the case of large signals. The distributed 20 MHz master clock signal enters the fourth input. A signal from the PMT anode triggers the ARS by crossing an amplitude threshold set to a fraction of the SPE average amplitude (the L0 threshold). The signal is time-stamped and its charge integrated to a precision of ∼10% to compensate for time walk effects. A time to voltage converter (TVC) interpolates between 20 MHz clock pulses to give a time resolution of ∼0.4 ns. Integrated charge and time stamp are then stored in the mixed analogue/digital pipeline memory. At the ARS output, an SPE tag consists of a header (1 byte), the integrated charge (1 byte), TVC (1 byte) and the time stamp (3 bytes).

In recent tests [13, 14] with signals from a PMT illuminated with mainly single photoelectrons at a single point on the photocathode, a time resolution of ∼1.1 ns has been achieved, comparing favourably with the PMT TTS of $\sigma \sim 1.3$ ns with full photocathode illumination. The intrinsic time resolution of the ARS was determined to be $\sigma \sim 350$ ps from measurement of the separation of two pulses injected into the ARS with a known time difference.

Analogue pulse shape discrimination separates SPE pulses, which are charge-integrated, from waveform (WF) pulse shapes, which are WF-sampled in 128 samples at up to 1 GHz. This processing is implemented when the pulse height exceeds several photoelectrons, when the time over the L0 threshold is longer than normal, or when the L0 threshold is crossed more than once in the charge integration time. With 128 analogue samples of the waveform, at the ARS output, a WF event can typically contain >250 bytes.

SPE events are expected to represent more than 98% of the ANTARES data, while WF events will be mainly generated by background phenomena, primarily ^{40}K disintegrations and bioluminescence. The pipeline memory of each ARS can store up to 16 SPE hits or 4 WF hits.

With a singles rate of 70 kHz, and 2% fraction of WF events, the (typical) data rate will be ∼7 Mbytes s^{-1} per PMT. Two ARS chips are connected to each PMT to reduce dead time. This data rate is shared between the (fast) output ports of the two ARSs and is well within the 20 Mbytes s^{-1} bandwidth limit of each. The PMT readout system is intended to handle an average singles rate of up to 100 kHz with surges of up to 250 kHz due to bioluminescence bursts.

Data from five PMT triplets (five levels) will be merged onto a single descendant fibre with a typical bandwidth of 105 Mbytes s^{-1}. Data from six such fibres will be dense wavelength division (DWD)-multiplexed onto a single fibre at the bottom of each detection line, resulting in a typical data rate to shore of 700 Mbytes s^{-1} per line. These fibres pass through the junction box and onto the 40 km electro-optical cable linking the detector array to the shore.

An on-shore data switchyard will de-multiplex up to 70 incoming data streams and pass data to a processing farm consisting of up to 100 PCs running at an input data rate in the range 50–100 Mbytes s^{-1}.

4.5.3. NEMO readout system R&D. The NEMO collaboration is studying a readout system for a km^3-scale array of 4096 PMTs. An event rate of 50 kHz per PMT (dark current + 40K + SPE signals + average bioluminescence contribution) has been assumed [11]. A PMT signal-processing ASIC ('LIRA01', built in AMS 0.35 μm CMOS technology: [11]) with three channels of 256-deep switched capacitor array analogue memory and 200 MHz sampling rate is under

development. The ASIC channels sample the PMT anode, a dynode and the 20 MHz master clock. LIRA01 will also incorporate a twin threshold (0.25 SPE, 5 SPE) discriminator trigger and single photon classifier. The ASIC is aimed at a temporal resolution of 300 ps. The DAQ output rate (after zero suppression and packing) is ∼5 Mbytes s^{-1}per PMT. Two LIRA ASICs will be used in each optical module: while one is sampling the PMT, the other will push data out towards a 20 MHz sampling ADC.

A synchronous digital hierarchy (SDH) protocol is being considered for data transmission and reception. An STM-1 tributary: (up to 155 Mbytes s^{-1}) might be used for the readout of a floor (4 PMTs) onto a single descending optical fibre. In electronics at the tower base, the 16 floor STM-1 streams would be multiplexed onto a single optical fibre running the STM-16 protocol (up to 2.5 Gbytes s^{-1}).

The array power and readout architecture envisions eight secondary junction boxes (SJBs) and a primary junction box (PJB) to which the shore electro-optical cable is connected. The principal data paths from the SJBs to the PJB follow a star network, with a redundant data ring between the SJBs. Data from each subarray of eight towers would be DWD-interleaved[15] in its SJB onto a single optical fibre, thence passing to the PJB (with the additional redundant highway between SJBs), before being retransmitted onto the 100 km shore electro-optical cable following a + 17 dB m amplification.[16]

4.6. Underwater acoustic survey and navigation

The reconstruction of muon tracks in an underwater neutrino detector is based on precise measurements (∼1 ns) of the arrival times of Čerenkov photons at optical modules. This reconstruction requires knowledge of the positions of the optical modules relative to each other or, more practically, with respect to fixed reference points such as the detector line anchors. The precision of this spatial positioning should be better than the corresponding dispersive uncertainty in the arrival time of Čerenkov light detection (e.g. ∼1.6 ns over a typical flight distance of 40 m in ANTARES). Since 1 ns is equivalent to 22 cm of light travel path in water, the relative position of every OM should be known to ∼10–20 cm.

Since detection lines will be suspended between sea anchors and submerged buoys subject to movement by deep ocean currents, the positions of individual optical modules will need to be regularly determined from measurements of line curvature and twist. In ANTARES, the relative positions of the OMs will be obtained from fits to position data determined by two independent systems: a high-frequency long base line LBL acoustic system [14, 15] and a series of semiconductor tiltmeter-compass sensors disposed along each detection line. The relative positions of the OMs will then be deduced from this reconstructed line shape and from the geometry of the OM frame. Additionally, a network of laser and LED beacons producing narrow, time-stamped blue light flashes will be used to give redundancy in the on-line calibration of PMT timing.

4.6.1. The ANTARES acoustic positioning system. An array of four 40–60 kHz acoustic transponders [15][17] delineating a 300 × 300 m LBL square, has been deployed on the seabed at

[15] Candidate device: AWG/CI008 by E-Tek Dynamics.
[16] Candidate device: type 1738U Erbium-doped Fiber Amplifier by Agere Systems.
[17] Frequency range 44–60 kHz, 2 kHz channel spacing (Genisea/ECA, Toulon, France).

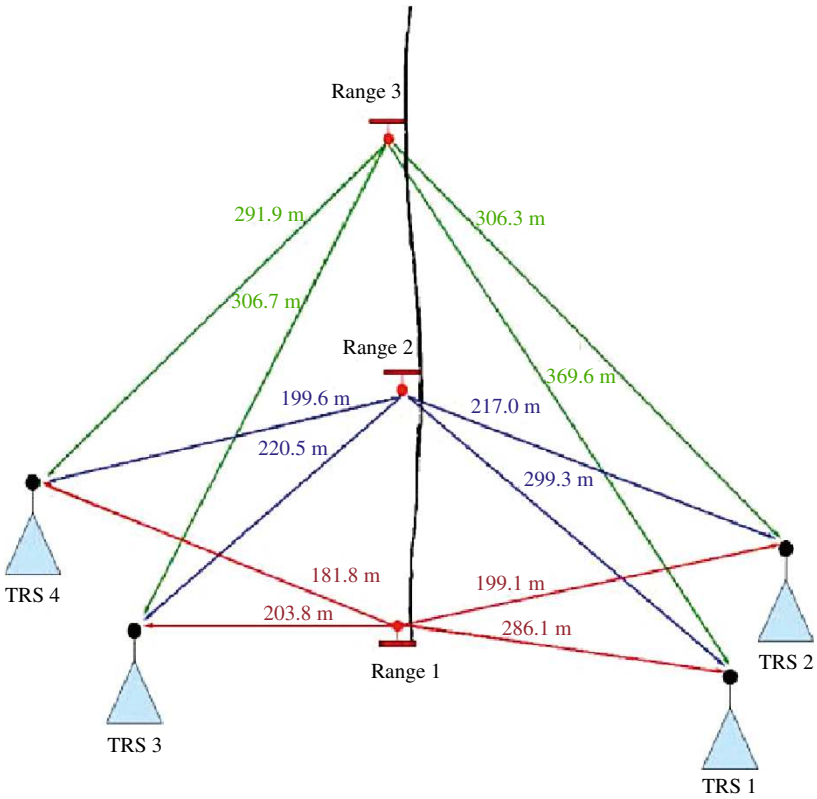

Figure 17. Illustration of relative positions of hydrophone rangefinders and transponders.

the ANTARES site. Additional transponders will be added (on sea anchors) as detection lines are deployed. The LBL transponders will transmit sound signals to hydrophones mounted at six positions (altitudes 100, 184, 256, 328, 388 and 448 m) along each detection line. The 3D positions of the hydrophones will be obtained by triangulation. The seabed transponders will interrogate each other and the seabed anchors to determine their relative positions. Figure 17 illustrates a recent implementation of the acoustic survey system with rangemeter hydrophones at three elevations on a deployed line. The precision of vertical height measurement between two hydrophone rangemeters was measured to be better than 5 cm as can be seen in figure 18. The transmission and reception of each sound pulse must be time-referenced relative to the master clock signal used to time-stamp PMT data. The conversion of acoustic transit times to distances requires accurate knowledge of the sound velocity within the detector. This in turn depends on the temperature, salinity and pressure [16].

Instrumentation to monitor these parameters will be needed, and has been extensively studied in the ANTARES-NEMO collaboration. These instruments are included on a dedicated instrumentation line.

4.6.2. Semiconductor tiltmeter/compass systems. The detection lines of ANTARES will incorporate combined bi-axial tiltmeter and compass sensors[18] to give the localtilt angles of

[18] Model TCM2-20 (Precision Navigation Inc., Santa Rosa, CA, USA; http://www.pnicorp.com).

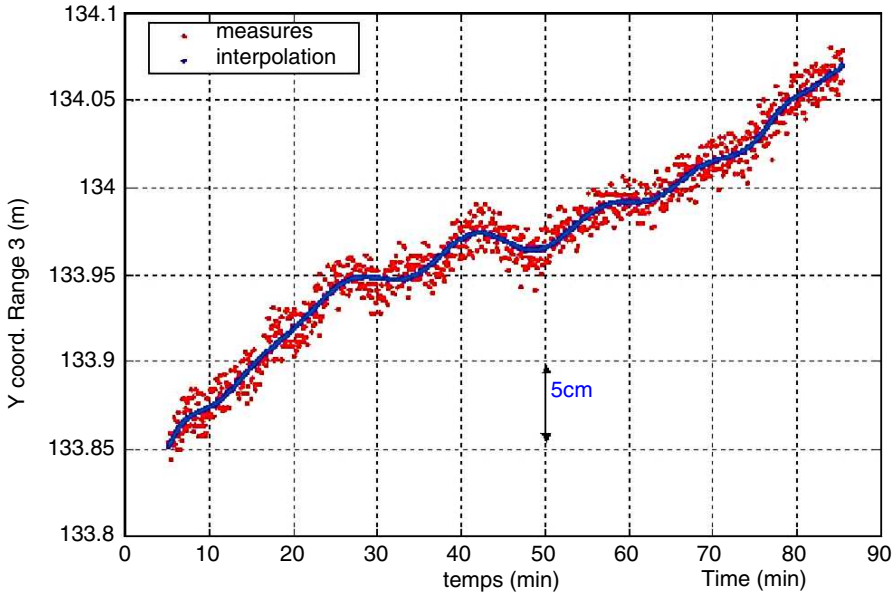

Figure 18. Time variation of vertical displacement between hydrophone rangefinders due to deep ocean current.

each OM triplet level with respect to the horizontal plane (range/precision; $\pm 20/\pm 0.2^\circ$ in pitch and roll), as well as its orientation relative to Earth Magnetic North (heading range/precision; $0\text{–}360^\circ/\pm 0.5 \rightarrow 1^\circ$), caused by cable torsion.

The performance of the positioning system has been studied in various configurations (varying the number of acoustic sensors and tiltmeters; the locations and precision of sensors, positions of missing sensors, etc), with differing values of deep water current and detector line twist as a function of altitude. These studies indicate that the proposed combination of acoustic triangulation and tiltmeter compasses should allow the positions of all OMs to be determined with an accuracy $\sigma < 10\,\text{cm}$ in deep water currents up to $15\,\text{cm}\,\text{s}^{-1}$.

4.7. Site evaluation and underwater and environmental instrumentation

NEMO and ANTARES, together with the Lake Baikal experiment, have a common programme of site measurements and instrument cross-calibration [4, 17]. Some instruments have been used at all three sites. Additionally, many of the results from the instruments used in site characterization are of interest to the oceanographic, deep-sea biology and geophysics communities. The NESTOR collaboration has, for example, been acquiring real-time seismograph and ocean current data at its Ionian Sea site since January 2002. The NEMO test site lab at Catania will acquire real-time data from the GEOSTAR-Poseidon underwater seismic station.

One output of the ANTARES junction box (two conductors at 500 V ac, and four optical fibres; DAQ Tx, Rx and two carrying GPS-referenced clocks) will be made available for oceanographic collaborators, while on another output a comprehensive array of environmental monitoring instruments for the ANTARES site, some developed by the NEMO collaboration, will be incorporated onto a dedicated instrumentation line.

4.7.1. The ANTARES instrumentation line. One of the 16 junction box outputs will be reserved for an 'instrumentation line' containing equipment for monitoring the detector array and

deep-sea environmental parameters including salinity, sound velocity, water transparency and current profile. For detector-wide timing calibration, a laser beacon will illuminate the array with fast (900 ps), time-stamped laser[19] pulses at a wavelength of 456 nm. Its action will complement shorter-range blue LED beacons distributed among the detection lines.

The deep-sea current profile (velocity, direction) will be sampled over 256 intervals over the full detector depth of 300 m by a pair of 300 kHz acoustic Doppler current profilers[20] with a velocity range (resolution) of 5 m s^{-1} (1 mm s^{-1}).

The optical attenuation of water at 470 nm will be measured over a 25 cm path length using a commercial photodiode-based water transmission meter.[21] The line will be equipped with sound velocity meters of the same type as installed close to the sea anchors of some detection lines. These devices[22] have a flight path of 20 cm and a precision of ± 0.05 m s^{-1} for typical velocities in the range 1400–1600 m s^{-1}. Several velocity meters will also be equipped with conductivity–temperature[23] and depth (pressure) probes.[24] A seismometer will also be connected to the instrumentation line. A preliminary version of the instrumentation line with a single current profiler, shown in figure 19, was deployed in early 2003.

4.8. Sea deployment and recovery operations

An essential feature of undersea neutrino telescopes is the necessity to have access to significant naval resources. These naval resources include surface boats and structures together with submersible vehicles of different types. The three Mediterranean projects have taken very different detector design choices implying the need for different naval resources; in particular, NESTOR wishes to avoid the necessity for undersea vehicles while ANTARES and NEMO choose to use them. The success of the two projects currently building detectors will in large part be conditioned by these choices and the naval resources used.

4.8.1. ANTARES deployment procedures. Table 2 illustrates the equipment necessary in the installation and repair of the ANTARES detector array which is centred on a junction box linked to a shore cable.

Connections of underwater detection lines require the plugging of cables with underwater-mateable connectors through the use of a manned submarine or ROV. In all cases, an already-deployed seabed acoustic transponder net and a ship with a GPS-referenced dynamical positioning system are required. Objects to be deployed on the seabed are equipped with their own acoustic transponders, allowing their positions to be triangulated with respect to an already deployed acoustic transponder net, of which the ANTARES LBL is an example.

During the deployment of the ANTARES junction box at a depth of 2400 m, the undersea electro-optical cable was first located through shop-borne interrogation of the acoustic

[19] Incorporating a NG-10120-120 laser head (Nanolase, Meylin, France).
[20] Workhorse Monitor (RD Instruments, San Diego, CA, USA).
[21] C-STAR (WETlabs Inc.; http://www.wetlabs.com).
[22] Model QUUX-3A(A) (Genisea, France).
[23] OEM-OT sensor by Falmouth Scientific (Cataumet, MA, USA; http://www.falmouth.com; precision of ± 0.001 mS cm^{-1}).
[24] Druck S A (Asnières sur Seine, France).

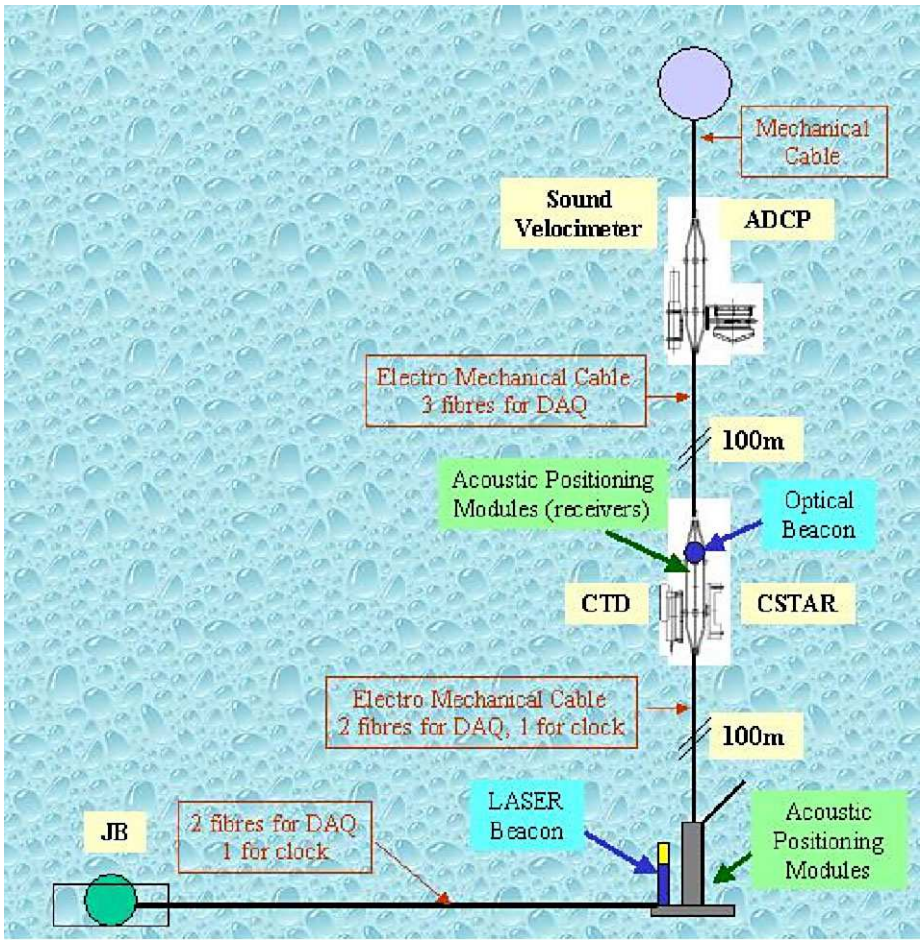

Figure 19. Configuration of a prototype instrumentation line to be deployed at the ANTARES site.

Table 2. Resources required for detector installation and detector repairs in ANTARES.

	Underwater resource required		
Deployed object	GPS/acoustic navigation	Grapple	Submarine vehicle
(a) *Detector installation*			
Shore site E/O cable	YES	NO	NO
Junction box	YES	YES	NO
Detection line	YES	NO	NO
Line-JB cable connect	YES	NO	YES
(b) *Detector repairs*			
Shore site E/O cable	YES	YES	NO
Junction box	YES	YES	YES
Detection line	YES	NO	NO
Line-JB cable connect	YES	NO	YES

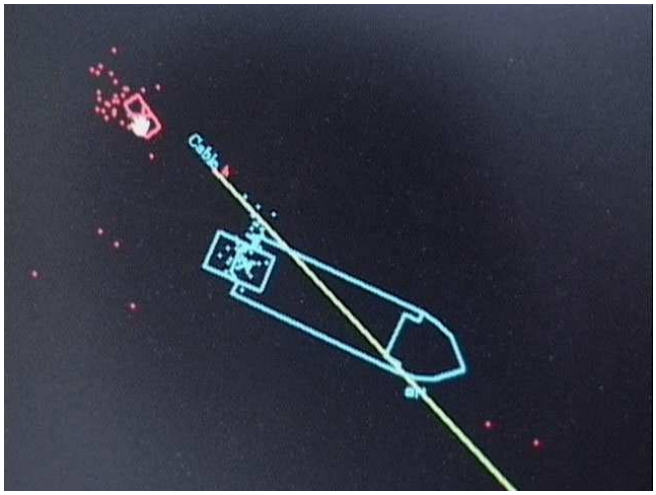

Figure 20. Acoustic transponder positioning of the ANTARES junction box during descent to seabed.

transponder attached to its 400-m-long dredging tail. Movement of this transponder confirmed when the lowered grapple had successfully snagged the dredging tail. The descent of the junction box to the seabed was monitored in real time by triangulation of the position of its individual acoustic transponder relative to the deployed LBL net.

In figure 20, the most recent position of the junction box is shown by a rectangle, while previous positions (at differing heights) are indicated by spots. During the descent, the dynamical positioning ship adjusted its position 2.5 km along the track of the undersea cable as 2.5 km of cable were re-laid on the seabed with the junction box attached.

4.8.2. NESTOR deployment procedures. In contrast, the NESTOR array will be deployed without the need for ROVs to perform underwater cable connections. Instead, underwater connections require that the last 5 km of the underwater cable from the shore station be raised with the seafloor instrument package. Several times in tests, the collaboration has deployed and recovered payloads composed of its base station and several floors from a depth of 4000-m using cable-laying ships or platforms. The collaboration is constructing a highly specialized deployment platform. The self-propelled and ballasted platform shown in figure 21 has an equilateral triangular form of side 51 m, with a central well. It will be equipped with a GPS-related dynamical positioning system capable of maintaining its position at sea to a precision of several metres, and can be used to deploy structures with diameters as large as 100 m.

Figure 22 illustrates the NESTOR deployment/recovery concept [18] using a 5000 m neutral buoyancy (recovery rope, ReRo) rope equipped with an anchor, buoy and acoustic release at its free end. During deployment, a NESTOR tower is lowered to the sea bottom (together with the final 5 km of undersea cable) and the ReRo is laid across the sea floor with its anchor and buoy positioned around 5 km from the tower base. During recovery the ReRo anchor is released with a coded acoustic signal and the buoy floats to the surface for capture. Once the 5000 m ReRo has been winched aboard the ship the tower will be at the surface for connection of additional floors or the removal or replacement of components.

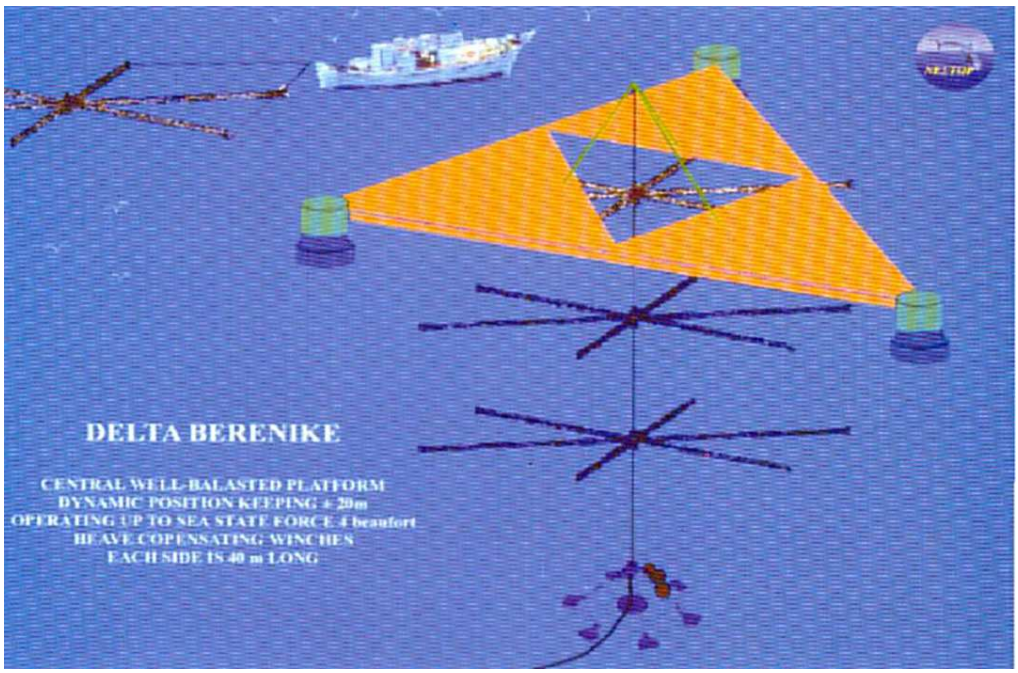

Figure 21. NESTOR deployment platform.

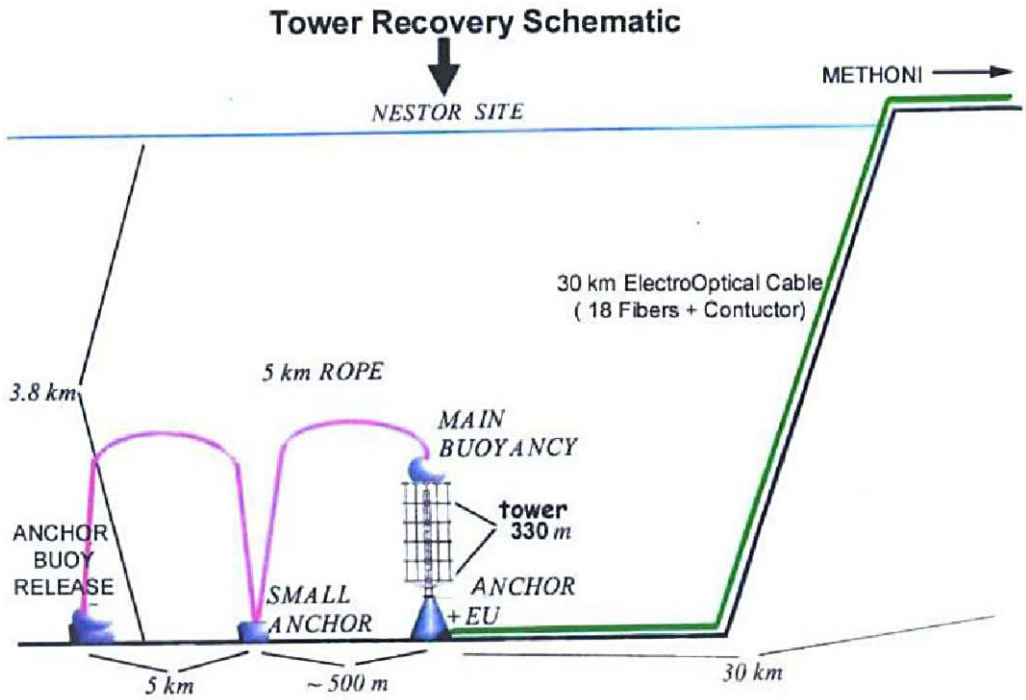

Figure 22. NESTOR tower deployment and recovery using a 5 km recovery rope.

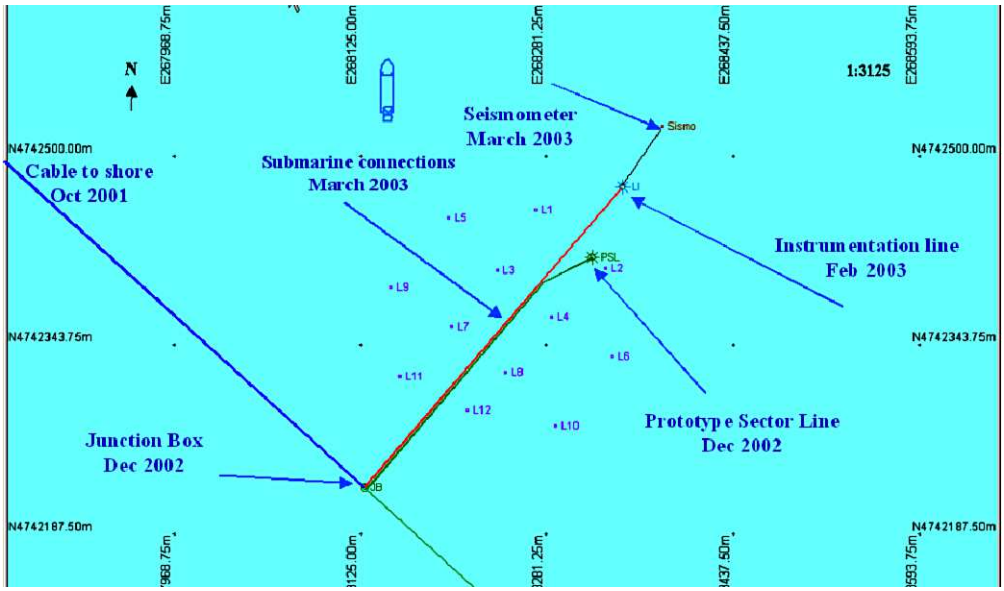

Figure 23. Configuration of ANTARES Telescope on seabed March 2003. The Shore cable and Junction Box installations are permanent. The MIL was recovered in May 2003 and the PSL was recovered in July 2003.

5. Status in spring 2004

ANTARES and NESTOR which have finished their R&D activities and the prototype stages are now in the process of full detector construction. NEMO is continuing R&D towards a km^3 detector.

5.1. ANTARES construction status

In October 2001, the first permanent element of the ANTARES telescope, the submarine cable of length 45 km, was laid between the site and the beach of Les Sablettes in La Seyne-sur-Mer. On land, the electrical energy for the detector is supplied from a power supply in a cabin close to the beach and the optical fibre continue to the shore station in the Institute Michel Pasha at a distance of 45 km. In December 2002, the junction box was connected to the cable and deployed on the seabed.

During 2002, a final short prototype optical line, prototype sector line (PSL), and a prototype instrumental line, mini instrumentation line (MIL), were constructed and extensively tested in a dark room in the laboratory. The two lines were deployed and connected on the ANTARES site in sea operations between December 2002 and March 2003. Figure 23 illustrates the items deployed on the ANTARES site up to March 2003.

Following the line connections, data taking started with both of the lines functioning successfully. Extensive data were taken with the PSL until July 2003 when it was recovered. The MIL developed a water leak and was recovered in May after 1 month of operation.

The prototype testing showed a number of problems during the sea operation and these have been diagnosed in the laboratory after the line recoveries. The water leak in the MIL was due to a type of commercial connector which we now believe has a design fault; for the future, the corrective action will be to avoid using this type of connector. In both lines, there were faults in

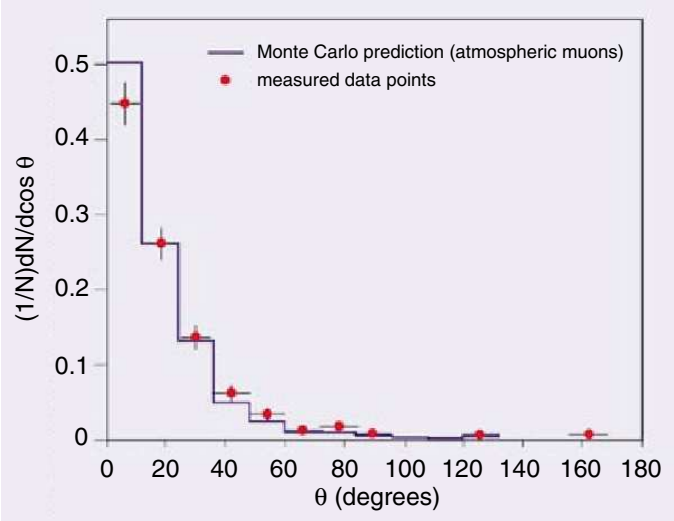

Figure 24. Comparison between the measured zenith angular distribution of muon tracks reconstructed in the NESTOR floor and the expected distribution.

the distribution in the line of the time reference clock due to broken optical fibres. The cause of the broken fibre is understood as the use of a substandard plastic tube in the line cables; for the future, steel tubes will be used to protect the optical fibres.

The background light levels in an undersea neutrino telescope are dominated from radioactive decay of ^{40}K in the sea-water salt and from bioluminescence. During the operation of the PSL the rates of background light from bioluminescence were higher than the values measured during the initial site explorations in which the measurements were made with autonomous mooring lines which recorded PMT counting rates in a memory. Following the evaluation of the data from the PSL tests, it is concluded that averaged over a year of operation of the full detector the data loss due to the bioluminescence would be 10–20% in neutrino detection efficiency.

The next step in the construction of the ANTARES telescope will be the installation of a new instrumentation line towards the end of 2004. Many elements of the full detector such as optical modules, mechanical structure and line cables are in production while the full orders for the electronics of the system will be placed in mid-2004. The installation of the full 12 lines of the detector will take place during 2005 and 2006. It is expected that the first exciting science results of the detector, opening up this new field of astroparticle physics in the northern hemisphere, will be available during 2006.

5.2. NESTOR status

At the end of March 2003 the first floor of a NESTOR tower was deployed at a depth of 4100 m. More than 5 million events consisting of a 4-fold coincidence between signals in the optical modules were recorded [19]. These data have been analysed in order to reconstruct muon tracks. The distribution of muons is shown in figure 24 compared with the predictions from flux calculations [20] using the Monte Carlo simulation of the detector. After operation of the floor for a period of time a fault developed in the submarine cable, which is now awaiting repair or replacement. The NESTOR collaboration plans to continue installation of the first tower during 2004.

6. Conclusion

The three Mediterranean projects have all made very significant progress in recent years. ANTARES and NESTOR will have completed detectors in the next few years. Together with the NEMO group they have combined in the 'KM3NET' design project for the next stage towards a km^3 Mediterranean Neutrino Telescope.

References

[1] Amram P *et al* 2003 *Astropart. Phys.* **19** 253
[2] Amram P *et al* 2000 *Astropart. Phys.* **13** 127
[3] Anassontzis E *et al* 1994 *Nucl. Instrum. Methods* A **349** 242
[4] Capone A 2002 *ANTARES Collaboration Meeting, Catania, 24–28 September*
[5] Sedita M 2002 *ANTARES Collaboration Meeting, Catania, 24–28 September*
[6] Hallewell G 2002 *ICFA Instrument. Bull.* **25** 17
[7] Amram P *et al* 2002 *Nucl. Instrum. Methods* A **484** 369
[8] Anassontzis E *et al* 2002 *Nucl. Instrum. Methods* A **479** 439
[9] Tzamarias S *et al* 2002 *Proc. 4th Workshop on Ring Imaging Čerenkov Detectors (RICH 2002), Pylos, June*
Tzamarias S *et al* 2003 *Nucl. Instrum. Methods* A **502** 150
[10] Musumeci N 2002 *ANTARES Collaboration Meeting, Catania, 24–28 September*
[11] Lo Nigro L 2002 *ANTARES Collaboration Meeting, Catania, 24–28 September*
[12] Druillole F *et al* 2001 *Proc. IEEE Symp. on Nuclear Science, 4–10 November, San Diego, CA*
[13] Feinstein F 2002 *Proc. 3rd Conf. on New Developments in Photo-detection, Beaune, June*
Feinstein F 2003 *Nucl. Instrum. Methods* A **504** 258
[14] Hallewell G 2002 *Proc. 4th Workshop on Ring Imaging Čerenkov Detectors (RICH 2002), Pylos, June*
Hallewell G 2003 *Nucl. Instrum. Methods* A **502** 258
[15] Bertin V, Genisea 2000 *ANTARES Report 3INS0103B*
[16] Chen C and Millero F 1977 *J. Acoust. Soc. Am.* **62** 1129
[17] Schuller J-P 2002 *ANTARES Collaboration Meeting, Catania, 24–28 September*
[18] Anassontzis E G and Koske P 2003 *Sea Technol.* **44** 10
[19] Ball A and Tsirigotis A 2003 *CERN Courier* **43** 23
[20] Okuda A 1994 *Astropart. Phys.* **2** 393